



ELSEVIER

Available online at [www.sciencedirect.com](http://www.sciencedirect.com)

SCIENCE @ DIRECT®

Nuclear Instruments and Methods in Physics Research B 230 (2005) 118–124

**NIM B**  
Beam Interactions  
with Materials & Atoms

[www.elsevier.com/locate/nimb](http://www.elsevier.com/locate/nimb)

## Energy loss of $H^+$ and $He^+$ in the semiconductors GaAs, ZnSe, InP and SiC

Santiago Heredia-Avalos <sup>a</sup>, Juan Carlos Moreno-Marín <sup>b</sup>,  
Isabel Abril <sup>c,\*</sup>, Rafael Garcia-Molina <sup>a</sup>

<sup>a</sup> *Departamento de Física, Universidad de Murcia, Apartado 4021, E-30080 Murcia, Spain*

<sup>b</sup> *Departament de Física, Enginyeria de Sistemes i Teoria del Senyal, Universitat d'Alacant, Apartat 99, E-03080 Alacant, Spain*

<sup>c</sup> *Departament de Física Aplicada, Universitat d'Alacant, Apartat 99, E-03080 Alacant, Spain*

Available online 21 January 2005

### Abstract

We have theoretically studied the electronic stopping cross section and the energy loss straggling of swift light ions ( $H^+$  and  $He^+$ ) moving through several compound semiconductors (GaAs, ZnSe, InP and SiC) as a function of the incident projectile energy. The calculations have been done using the dielectric formalism, in which the electronic structure of the projectile is described by the modified Brandt–Kitagawa model and the energy loss function (ELF) of the semiconductors is obtained using a linear combination of Mermin-type ELF to describe the outer electron excitations and generalized oscillator strengths to take into account the excitations of the inner-shell electrons. The different charge states that the projectile can acquire during its travel through the solid, as a result of electronic capture and loss processes, has been also considered. The contributions to the projectile energy loss from both the outer- and the inner-shell electron excitations are analyzed. The comparison of our calculated stopping cross sections with available experimental data shows a good agreement in a wide range of incident projectile energies.

© 2004 Elsevier B.V. All rights reserved.

*PACS:* 34.50.Bw; 77.22.–d; 47.27.Vf; 61.46.+w

*Keywords:* Stopping power; Proton energy loss; Dielectric properties of semiconductors

The energy loss of ions in matter is an interesting topic since its study offers both basic and technological possibilities, improving our knowledge

about the structure of matter or allowing a controlled modification of the material properties [1]. Accurate stopping power values are required in the processing of materials by ion beam implantation as well as in the structural characterization of solids by ion beam methods, since the depth scales of the samples implanted or characterized by ion

\* Corresponding author. Tel.: +34 65 909578; fax: +34 65 903464.

E-mail address: [ias@ua.es](mailto:ias@ua.es) (I. Abril).

beam techniques are based mainly on the slowing down of these ions in the sample material. Thus, it is desirable to have theoretical frameworks that reproduce and predict the energy loss of ions in a wide range of projectile energies and for different types of target materials.

In this work, we study theoretically the energy loss of swift  $H^+$  and  $He^+$  ion beams in several compound semiconductors (GaAs, ZnSe, InP and SiC) because the potential applications of these materials, specially in microelectronics [2,3]. Our model is based on the dielectric formalism, where the projectile charge density is described using the modified Brandt–Kitagawa model [4] and the dielectric properties of the target are modelled in a realistic way [5,6]. The different charge states that the projectile can acquire inside the target due to electron capture and loss processes is also considered. It is worth to notice that we only take into account the energy loss due to the excitations of the target electrons because the nuclear energy loss is negligible for the projectile energy range used here. In what follows we will use atomic units, except where otherwise stated.

When a projectile with velocity  $v$  travels through a target, it can change its charge state due to electron capture and loss processes, then the stopping power  $S_p$  (or the energy loss straggling  $\Omega^2$ ) of a solid will be a sum of the stopping power contributions  $S_{p,q}$  (or the energy loss straggling contributions  $\Omega_q^2$ ) due to the different charge states  $q$  that the projectile can acquire, that is,

$$S_p = \sum_{q=0}^{Z_1} \phi_q S_{p,q}, \quad \Omega^2 = \sum_{q=0}^{Z_1} \phi_q \Omega_q^2, \quad (1)$$

where  $Z_1$  is the projectile atomic number and  $\phi_q$  is the fraction of the  $q$  charge state, which depends on the target, the projectile and its velocity (in what follows we use  $\phi_q$  values obtained by the code CasP 3.0 [7]). Note that the summations are extended over all the possible charge states of the projectile.

The stopping power for a given charge state  $q$  of the projectile,  $S_{p,q}$ , is evaluated using the dielectric formalism, which is based on a linear response of the stopping medium to the perturbation produced by the projectile charge density [8]

$$S_{p,q} = \frac{2}{\pi v^2} \int_0^\infty dk \frac{\rho_q^2(k)}{k} \int_{E_g}^{kv} d\omega \omega \text{Im} \left[ \frac{-1}{\epsilon(k, \omega)} \right], \quad (2)$$

where  $k$  and  $\omega$  are, respectively, the momentum and energy transferred to the target,  $E_g$  is the energy gap of the semiconductor,  $\rho_q(k)$  is the Fourier transform of the projectile charge density for the  $q$  charge state, and  $\text{Im}[-1/\epsilon(k, \omega)]$  is the energy loss function of the target, which determines its response to external perturbations.

In a similar way, the energy loss straggling for a given charge state  $q$  of the projectile,  $\Omega_q^2$ , can be obtained like in Eq. (2) but replacing  $d\omega \omega$  by  $d\omega \omega^2$ .

The charge density of the projectile is described by the model proposed by Brandt and Kitagawa [9] but considering the modification proposed in [4] because the bound electrons of the projectile are in the K-shell. The energy loss function of the target is modelled through a linear combination of Mermin-type [10] ELF to take into account the external electron excitations, and by generalized oscillator strengths (GOS) to describe the inner-shell electron excitations of the target [5,6]. This method has been successfully applied to calculate the proton energy loss in several elemental [11–13,6] and compound [5] targets. The procedure to build the ELF consists in a fitting to the experimental spectrum of the ELF in the optical limit (momentum transfer  $k = 0$ ) for a wide range of transferred energies

$$\begin{aligned} & \text{Im} \left[ \frac{-1}{\epsilon(k=0, \omega)} \right]_{\text{outer electrons}} \\ &= \sum_i A_i \text{Im} \left[ \frac{-1}{\epsilon_M(k=0, \omega; \omega_i, \gamma_i)} \right]_{\omega \geq E_{th,i}}. \end{aligned} \quad (3)$$

The fitting parameters  $\omega_i$ ,  $\gamma_i$  and  $A_i$  are related, respectively, with the position, the width and the intensity of the peaks and other structures observed in the target ELF, and  $E_{th,i}$  is a threshold energy. The subindex in  $\epsilon_M$  appearing in the right-hand side of Eq. (3) refers to the Mermin procedure [10] to construct the dielectric function.

The excitations of the inner-shell electrons are described in terms of the generalized oscillator strengths for isolated atoms; this approach is

suitable since inner-shell electrons have large binding energies and show negligible collective effects. The relation between the ELF and the GOS is given by [14]

$$\text{Im} \left[ \frac{-1}{\epsilon(k, \omega)} \right]_{\text{inner electrons}} = \frac{\pi \omega_{p0}^2}{2\omega} \frac{df(k, \omega)}{d\omega}, \quad (4)$$

where  $df(k, \omega)/d\omega$  is the GOS per unit excitation energy and  $\omega_{p0}$  is the plasmon energy corresponding to one free electron per atom. We employ the hydrogenic approach for the GOS because it gives realistic values of the inner-shell ionization cross sections [1,14].

According to [5,6], the fitting parameters ( $\omega_i$ ,  $\gamma_i$ ,  $A_i$ ) of the energy loss function are chosen in such manner that they verify the  $f$ -sum rule for the effective number of electrons in the target. Note that the Mermin dielectric functions safeguard the fulfilment of the  $f$ -sum rule for all momentum transferred, if it is satisfied for  $k=0$ . Also, as an additional checking we calculate the mean excitation energy of the target.

Since the description presented here for the ELF contains all the relevant information on the electronic transitions and band structure effects in the optical range and a consistent extension to the whole  $(k, \omega)$ -range, it is expected that this model should provide a realistic description of the energy loss spectra for each particular target. However, for some materials, in special for compounds, there are not experimental ELF data in the optical limit for a wide range of excitation energies. Therefore for large values of  $\omega$ , we construct the ELF of a compound  $A_xB_y$  from the ELF of its elementary constituents, A and B, applying the additivity of their respective ELF/ $n$  ratios, where  $n$  is the atomic or molecular density of the target, that is,

$$\frac{\text{ELF}(A_xB_y)}{n(A_xB_y)} = x \frac{\text{ELF}(A)}{n(A)} + y \frac{\text{ELF}(B)}{n(B)}. \quad (5)$$

Although the results obtained using Eq. (5) would not be reliable for energies corresponding to the excitation of the valence electrons, they are correct for energies comparable to that of the inner shells, since only the external electrons of the atoms participate in the formation of the compound, and the inner shells remain practically insensitive to this process.

In Fig. 1 we show the ELF at  $k=0$  of GaAs, ZnSe, InP and SiC semiconductors as a function of the transferred energy. For each target, the solid line corresponds to our fitting based on Eqs. (3)–(5), the left side of the figure being the ELF due to excitations of the most outer electrons, whereas the right side, in a logarithm scale, represents the ELF due to the excitations of the inner-shell electrons. The parameters  $\omega_i$ ,  $\gamma_i$ ,  $A_i$  and  $E_{th,i}$  used to fit the contribution of the external electrons to the ELF, Eq. (3), appear in Table 1. The experimental data of the ELF for each semiconductor are represented by symbols [15]. For higher energies, where experimental data are not available, the ELF of the compound is calculated according to Eq. (5), where the ELF of each element is obtained from X-ray scattering factors [16]. The ELF at  $k=0$  of these compound semiconductors

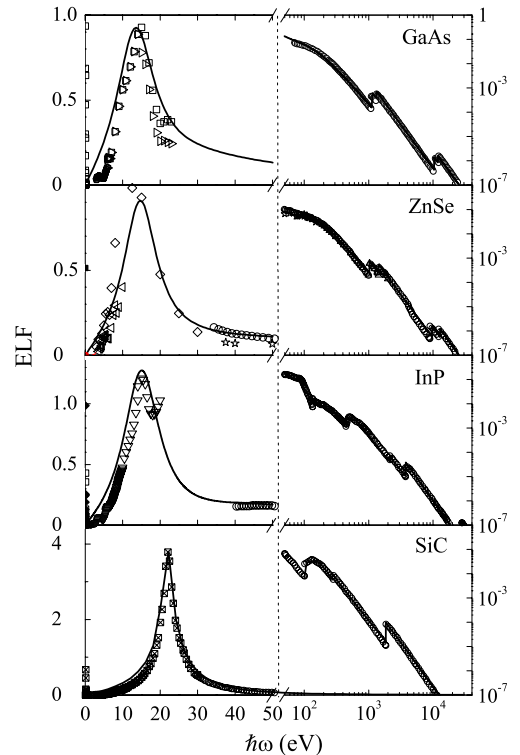


Fig. 1. Energy loss function at  $k=0$  of GaAs, ZnSe, InP and SiC, as a function of the excitation energy. The solid line represents our fitting to the experimental ELF (denoted by symbols [15]) and the reconstructed ELF applying Eq. (5) to the X-ray scattering factors [16] (represented by  $\circ$ ).

Table 1

Parameters used to fit the optical ELF corresponding to the outer electrons (Eq. (3)) of GaAs, ZnSb, InP and SiC

Target	$i$	$E_{\text{th},i}$ (eV)	$\hbar\omega_i$ (eV)	$\hbar\gamma_i$ (eV)	$A_i$
<b>GaAs</b> $\rho = 5.316 \text{ g/cm}^3$ $E_g = 1.35 \text{ eV}$	1	0	14.7	12.2	$6.54 \times 10^{-1}$
	2	0	38.1	62.6	$1.75 \times 10^{-1}$
	3	0	117	212	$7.12 \times 10^{-2}$
<b>ZnSe</b> $\rho = 5.42 \text{ g/cm}^3$ $E_g = 2.58 \text{ eV}$	1	0	15.6	10.9	$5.62 \times 10^{-1}$
	2	0	54.42	163	$1.06 \times 10^{-1}$
	3	0	108	201	$9.09 \times 10^{-2}$
<b>InP</b> $\rho = 4.787 \text{ g/cm}^3$ $E_g = 1.27 \text{ eV}$	1	0	16.1	11.4	$8.62 \times 10^{-1}$
	2	0	53.1	51.7	$1.31 \times 10^{-1}$
	3	0	84.4	20.4	$1.46 \times 10^{-2}$
	4	135	245	272	$4.69 \times 10^{-3}$
	5	444	599	517	$1.45 \times 10^{-3}$
<b>SiC</b> $\rho = 3.217 \text{ g/cm}^3$ $E_g = 2.3 \text{ eV}$	1	0	22.0	3.5	$4.57 \times 10^{-1}$
	2	0	23.4	16.3	$6.76 \times 10^{-1}$
	3	101	158	128	$2.38 \times 10^{-2}$

shows the following general features: the structure of the ELF is determined by interband transitions at low transferred energies while the highest maximum is ascribed to the excitation of volume plasma oscillations. We also notice that the electrons of each target atom that do not participate in the molecular binding clearly appear as an abrupt peak in the ELF for high transferred energies. We have used GOS to describe the excitations of the K-inner shell electrons for light target atoms (C, Si and P) and of the K- and L-inner shell electrons for intermediate target atoms (Zn, Ga, As, Se and In).

On the other hand, we have calculated the mean excitation energy,  $I$ , according to [17] for each semiconductor and we have obtained:  $I(\text{GaAs}) = 339 \text{ eV}$ ,  $I(\text{ZnSe}) = 346 \text{ eV}$ ,  $I(\text{InP}) = 372 \text{ eV}$  and  $I(\text{SiC}) = 162 \text{ eV}$ ; unfortunately there are not experimental data of the mean excitation energy for these compound materials. The application of Bragg's rule [18] to  $I$  gives the following values:  $I^{\text{Bragg}}(\text{GaAs}) = 385 \text{ eV}$ ,  $I^{\text{Bragg}}(\text{ZnSe}) = 384 \text{ eV}$ ,  $I^{\text{Bragg}}(\text{InP}) = 432 \text{ eV}$  and  $I^{\text{Bragg}}(\text{SiC}) = 150 \text{ eV}$ ; it is worth to note that some  $I$  values corresponding to elementary targets are from interpolated data [19].

The stopping cross sections (SCS) of GaAs, ZnSe, InP and SiC for  $\text{H}^+$  and  $\text{He}^+$  are shown in

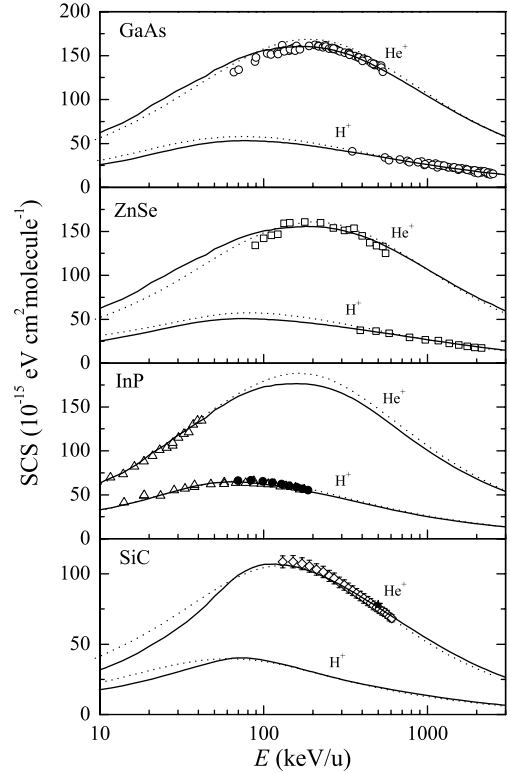


Fig. 2. Stopping cross section (SCS) of GaAs, ZnSe, InP and SiC for  $\text{H}^+$  and  $\text{He}^+$  as a function of the projectile energy. For each case, the solid line represents our calculations, the dotted lines are SRIM-2003 predictions [22], and the symbols refer to experimental data:  $\text{H}^+$  and  $\text{He}^+$  in GaAs ( $\circ$  [23]), in ZnSe ( $\square$  [24]),  $\text{H}^+$  in InP ( $\triangle$  [25] and  $\bullet$  [26]),  $\text{He}^+$  in InP ( $\triangle$  [25]) and  $\text{He}^+$  in SiC ( $\diamond$  [27] and  $\star$  [28]).

Fig. 2 as a function of the incident projectile energy. The solid lines represent our calculations and the symbols correspond to experimental data (see the figure caption). All the calculations presented have been done using the modified Brandt–Kitagawa model [4,9] to describe the electronic structure of the projectile. For a compound target, the fractions of each charge state of the projectile are obtained as the weighted average of the charge fractions given by the CasP 3.0 code [7] for each one of the constituent elements; the ELF of each semiconductor was described in the previous section and shown in Fig. 1.

The energy loss of swift  $\text{H}^+$  projectiles is calculated by a sum of the stopping power due to the different charge states that the projectile can

acquire,  $H^+$  and  $H^0$  (see Eq. (1)), but besides we include the energy loss associated to the electronic capture and loss processes,  $S_{CL}$ , and the polarization of the projectile [20], because they have special importance at low proton energies and near the SCS maximum.  $S_{CL}$  represents about  $\sim 5\%$  for GaAs and ZnSe and  $\sim 10\%$  for InP and SiC from the total SCS for a proton energy of 50 keV; these percentages diminish to  $\sim 3\%$  and  $\sim 5\%$ , respectively, when the proton energy increases to 100 keV. The inclusion of the projectile polarization rises the total SCS in  $\sim 5\%$  at a proton energy of 50 keV and  $\sim 2\%$  at 100 keV. For all the semiconductors considered (GaAs, ZnSe, InP and SiC) the agreement between our calculations of the SCS for  $H^+$  projectiles and the available experimental data are rather good.

Analogously, the total stopping cross section for helium projectiles is given by the contributions from the SCS for the different charge states ( $He^{2+}$ ,  $He^+$  and  $He^0$ ), weighted with the fractions corresponding to each charge state, see Eq. (1). In Fig. 2 we show, by a solid line, our calculated SCS of GaAs, ZnSe, InP and SiC for  $He^+$ , and the available experimental data, denoted by symbols (see the figure caption). In all the cases our results compare fairly well with the experimental data. The stopping cross section due to capture and loss of electrons by the projectile is not included in these calculations. However, the estimations proposed in [20] suggest that this phenomenon could contribute only about 5% over the total stopping cross section near its maximum; so despite this additional contribution to the SCS, our calculations still agree with the experimental data. On the other hand, we have checked that the contribution of the projectile polarization to the SCS is negligible because of the low polarizability of  $He^0$  and  $He^+$  [21].

For comparison, we have also plotted in Fig. 2 the semiempirical predictions of SRIM-2003 [22] based in a linear superposition of SCS of the atomic constituents of each target, without further corrections for chemical effects. The major discrepancy between our calculations and the SRIM-2003 curves appear at energies near and lower than the corresponding to the maximum SCS; these deviations can be ascribed to changes in the electronic

configuration of the target atoms when different compounds are formed. At high proton energies the differences with the SRIM-2003 code tend to disappear.

We have checked that the energy gap,  $E_g$ , of these semiconductors (see Table 1) does not affect the projectile energy loss for the projectile energy range considered here.

We have analyzed the contribution of the outer- and inner-shell electron excitations to the SCS of GaAs, ZnSe, InP and SiC for  $H^+$  and  $He^+$ . The main contribution to the SCS is obviously due to the outer electron excitations, however, when increasing the projectile energy the influence of the inner-shell electron excitations becomes more important. We find a similar influence of the inner-shell electron excitations in the SCS of GaAs and ZnSe for  $H^+$  and  $He^+$  due to their edge energies of their atomic components; in particular, the L-shell contribution of Ga and As in GaAs and Zn and Se in ZnSe represents  $\sim 5\%$  of the total SCS for a projectile energy of 1 MeV/u, whereas at 4 MeV/u it represents  $\sim 15\%$ ; however the K-shell contribution has no influence even at 4 MeV/u, for which it represents a contribution to the SCS less than 0.1%. For the case of InP target the contribution to the SCS due to the outer electron excitations is higher than 95% at a projectile energy of 4 MeV/u; in this case the K-shell of P and the L and K-shells of In have slight importance. For the SiC semiconductor, the K-shell of C contributes  $\sim 6\%$  to the total SCS for a projectile energy of 1 MeV/u, and for 4 MeV/u it represents  $\sim 10\%$ , whereas the K-shell of Si contributes  $\sim 1\%$  at 4 MeV/u.

We show in Fig. 3 the normalized energy loss straggling,  $\Omega^2/\Omega_B^2$ , of GaAs, ZnSe, InP and SiC for (a)  $H^+$  and (b)  $He^+$  as a function of the incident projectile energy. Bohr's energy loss straggling,  $\Omega_B^2$ , is a reference value valid at high projectile energies; we evaluate  $\Omega_B^2$  for a compound in a similar manner to Eq. (5), i.e. by adding the weighted ratios  $\Omega_B^2/n$  of their respective atomic constituents. Bohr's energy loss straggling for each monoatomic target is given by  $\Omega_B^2 = 4\pi Z_1^2 Z_2 n$ , where  $Z_1$  and  $Z_2$  are, respectively, the projectile and the target atomic numbers. At low projectile energies we obtain that the energy loss straggling is proportional

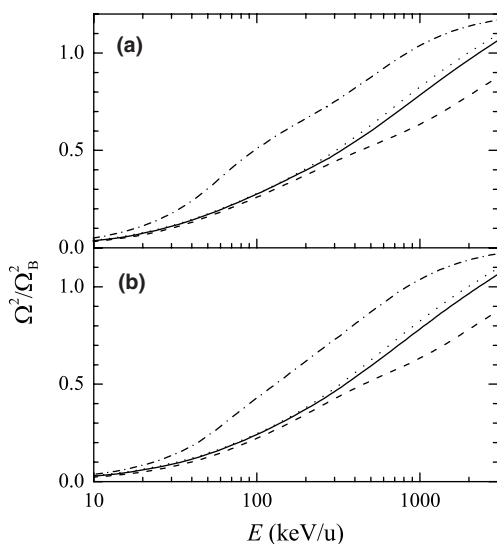


Fig. 3. Normalized energy loss straggling,  $\Omega^2/\Omega_B^2$  of GaAs (solid line), ZnSe (dotted line), InP (dashed line) and SiC (dash-dotted line) for (a)  $H^+$  and (b)  $He^+$  as a function of the incident projectile energy.

to the projectile energy. We can appreciate in Fig. 3 that energy loss straggling of these semiconductors for  $H^+$  and  $He^+$  tends to or exceed the Bohr's energy loss straggling at high projectile energies, when all the target electrons can be excited; this behavior, which can be attributed to the chemical effect, has been also obtained experimentally in the energy loss straggling of  $SiO_2$  for  $H^+$  [29].

In summary, we have presented a procedure to calculate the stopping cross section and the energy loss straggling of the compound semiconductors GaAs, ZnSe, InP and SiC, with interest in the microelectronic industry, for swift  $H^+$  and  $He^+$ . This procedure is based in the well known dielectric formalism, where the energy loss is evaluated taking into account the different charge state that the projectile can acquire in its travel through the target. The electronic structure of the projectile is described by the modified Brandt–Kitagawa model. The semiconductor's ELF is constructed in terms of a sum of Mermin-type ELF, to describe the outer electron excitations, and a GOS to take into account the inner-shell electron excitations; which are adjusted to reproduce the main characteristics of each material (experimental ELF in the optical limit, ionization energy  $I$ ,  $f$ -sum rule)

[5,6]. In the case of proton projectiles we also include the energy loss associated with the electron capture and loss processes and the polarization of the projectile. We have also analyzed the influence of the inner-shell electron excitations into the stopping cross section and we found that this contribution becomes to be important only at high projectile energies  $\geq 600$  keV/u.

We have compared our calculated stopping cross sections of semiconductors with available experimental data obtaining a satisfactory agreement in a wide range of projectile energies. We conclude that the method we have presented is suitable to predict the energy loss of swift light projectiles in compound materials with a complex electronic structures.

## Acknowledgements

This work was supported by the Spanish Ministerio de Ciencia y Tecnología (projects BFM2003-04457-C02-01 and BFM2003-04457-C02-02). SHA thanks the Fundación Cajamurcia for a postdoctoral research grant.

## References

- [1] M.A. Kumakhov, F.F. Komarov, Energy Loss and Ion Ranges in Solids, Gordon and Breach, New York, 1981.
- [2] I. Thurzo, L. Hrubcín, J. Bartos, E. Pincík, Nucl. Instr. and Meth. B 83 (1993) 145.
- [3] J. Raisanen, E. Rauhala, Nucl. Instr. and Meth. B 59–60 (1991) 592.
- [4] W. Brandt, Nucl. Instr. and Meth. 194 (1982) 13.
- [5] I. Abril, R. Garcia-Molina, N.R. Arista, C.F. Sanz-Navarro, Nucl. Instr. and Meth. B 190 (2002) 89.
- [6] J.C. Moreno-Marín, I. Abril, R. Garcia-Molina, Nucl. Instr. and Meth. B 193 (2002) 30.
- [7] P.L. Grande and G. Schiwietz, CasP. Convolution approximation for swift Particles, Version 3.0 (2004) code available from <http://www.hmi.de/people/schiwietz/casp.html>.
- [8] R. Garcia-Molina, S. Heredia-Avalos, I. Abril, J. Phys.: Condens. Matter 12 (2000) 5519.
- [9] W. Brandt, M. Kitagawa, Phys. Rev. B 25 (1982) 5631.
- [10] N.D. Mermin, Phys. Rev. B 1 (1970) 2362.
- [11] I. Abril, R. Garcia-Molina, N.R. Arista, Nucl. Instr. and Meth. B 90 (1994) 72.
- [12] D.J. Planes, R. Garcia-Molina, I. Abril, N.R. Arista, J. Electron Spectrosc. Relat. Phenom. 82 (1996) 23.

- [13] I. Abril, R. Garcia-Molina, C. Denton, F.J. Pérez-Pérez, N.R. Arista, *Phys. Rev. A* 58 (1998) 357.
- [14] R.F. Egerton, *Electron Energy-Loss Spectroscopy in the Electron Microscope*, Plenum Press, New York, 1989.
- [15] E.D. Palik, G. Ghosh (Eds.), *The Electronic Handbook of Optical Constants of Solids*, Academic Press, San Diego, 1999.
- [16] B.L. Henke, E.M. Gullikson, and J.C. Davis, *At. Data Nucl. Data Tab.* 54 (1993) No. 2, and from <http://xray.uu.se/hypertext/henke.html>.
- [17] E. Shiles, T. Sasaki, M. Inokuti, D.Y. Smith, *Phys. Rev. B* 22 (1980) 1612.
- [18] W.H. Bragg, R. Kleeman, *Philos. Mag.* 10 (1905) 318.
- [19] ICRU Report 37, *Stopping Powers for Electrons and Positrons*, International Commission for Radiation Units and Measurements, Bethesda, MD, 1984.
- [20] S. Heredia-Avalos, R. Garcia-Molina, *Nucl. Instr. and Meth. B* 193 (2002) 15.
- [21] K.P. Huber, in: B.H. Billins, H.P.R. Frederikse, D.F. Bleil, R.B. Lindsay, R.K. Cook, J.B. Marion, H.M. Crosswhite, M.W. Zemansky (Eds.), *American Institute of Physics Handbook*, McGraw-Hill, New York, 1972, p. 7.
- [22] J.F. Ziegler and J.P. Biersak, SRIM. The Stopping and Range of Ions in Matter, Version 2003.20 code available from [www.srim.org](http://www.srim.org).
- [23] M. Rajatora, K. Vakevainen, T. Ahlgren, E. Rauhala, J. Raisanen, K. Rakennus, *Nucl. Instr. and Meth. B* 119 (1996) 457.
- [24] K. Vakevainen, *Nucl. Instr. and Meth. B* 122 (1997) 187.
- [25] S.R. Lee, R.R. Hart, *Nucl. Instr. and Meth. B* 28 (1987) 470.
- [26] V.A. Khodyrev, V.N. Mizgulin, E.I. Sirotinin, A.F. Tulinov, *Radiat. Eff.* 83 (1984) 21.
- [27] Y. Zhang, W.J. Weber, *Appl. Phys. Lett.* 83 (2003) 1665.
- [28] E.E. Baglin, J.F. Ziegler, *J. Appl. Phys.* 45 (1974) 1413.
- [29] J.H.R. dos Santos, P.L. Grande, M. Behar, J.F. Dias, N.R. Arista, J.C. Eckardt, G.H. Lantschner, *Phys. Rev. A* 68 (2003) 042903.